CERN-TH/97-286
DTP/97/106
November 1997

QCD Analysis of Unpolarized and Polarized Λ - Baryon Production in Leading and Next-to-Leading Order

D. de Florian[a], M. Stratmann[b], W. Vogelsang[a]

[a] *Theoretical Physics Division, CERN, CH-1211 Geneva 23, Switzerland*

[b] *Department of Physics, University of Durham, Durham DH1 3LE, England*

Abstract

We analyze experimental data for the production of Λ baryons in e^+e^- annihilation in terms of scale dependent, QCD evolved, Λ fragmentation functions. Apart from the vast majority of the data for which the polarization of an observed Λ was not determined, we also consider the recent LEP measurements of the longitudinal polarization of Λ's produced on the Z-resonance. Such data correspond to spin-dependent fragmentation functions for the Λ. We point out that the present data are insufficient to satisfactorily fix these. We therefore suggest several different sets of fragmentation functions, all compatible with present data, and study the prospects for conceivable future semi-inclusive deep-inelastic scattering experiments to discriminate between them. We provide the complete next-to-leading order QCD framework for all the processes we consider.

1 Introduction

Measurements of rates for single-inclusive e^+e^- annihilation (SIA) into a specific hadron H,

$$e^+e^- \to (\gamma,\, Z) \to H\; X \quad , \tag{1}$$

play a similarly fundamental role as those of the corresponding crossed "space-like" deep-inelastic scattering (DIS) process $ep \to e'X$. Their interpretation in terms of scale-dependent fragmentation functions $D_f^H(z, Q^2)$, the "time-like" counterparts of the parton distribution functions $f_H(x, Q^2)$ of a hadron H, provides a further important, complementary test of perturbative QCD. In analogy with the "space-like" case, $D_f^H(z, Q^2)$ is the probability at a mass scale Q for finding a hadron H carrying a fraction z of the parent parton's momentum. QCD completely predicts the Q^2-dependence of the process-independent fragmentation functions $D_f^H(z, Q^2)$ via the Altarelli-Parisi evolution equations, once a suitable non-perturbative hadronic input at some initial reference scale μ has been determined from the data. So far, only the fragmentation into the most copiously produced light mesons (π, K) has been the issue of a thorough QCD analysis [1].

It is one of the purposes of this work to study along similar lines as in [1] whether such a formalism also applies to the production of Λ-baryons. Λ's are also produced at fairly large rates and, as for pions and kaons, the Q^2 range covered by present SIA experiments [2, 3] allows a detailed quantitative QCD analysis. Recently measured Λ production rates in semi-inclusive DIS (SIDIS) [4] provide an important testing ground for the fragmentation functions extracted from SIA data.

The production of Λ baryons appears to be particularly interesting also from a different point of view. Contrary to spinless mesons like pions and kaons, the Λ baryon offers the rather unique possibility to study for the first time spin transfer reactions. The self-analyzing properties of its dominant weak decay $\Lambda \to p\pi^-$ and the particularly large asymmetry of the angular distribution of the decay proton in the Λ rest-frame [5] allow an experimental reconstruction of the Λ spin. Over the past years "spin physics" has attracted an ever growing interest, as experimental findings [6] have not always matched

with "naive" theoretical expectations, the Gourdin-Ellis-Jaffe sum rule [7] being the most prominent example here. Studies of Λ polarization could provide a completely new insight into the field of spin physics whose theoretical understanding is still far from being complete despite recent progress, and they might also yield further information on the hadronization mechanism.

In [8] a strategy was proposed for extracting in SIA the functions $\Delta D_f^\Lambda(z,Q^2)$ describing the fragmentation of a longitudinally polarized parton into a longitudinally polarized Λ [9],

$$\Delta D_f^\Lambda(z,Q^2) \equiv D_{f(+)}^{\Lambda(+)}(z,Q^2) - D_{f(+)}^{\Lambda(-)}(z,Q^2) \quad , \tag{2}$$

where $D_{f(+)}^{\Lambda(+)}(z,Q^2)$ ($D_{f(+)}^{\Lambda(-)}(z,Q^2)$) is the probability for finding a Λ with positive (negative) helicity in a parton f with positive helicity (by taking the sum instead of the difference in (2) one recovers the unpolarized fragmentation function D_f^Λ). If the energy is far below the Z-resonance, one longitudinally polarized beam is required in order to create a non-vanishing net polarization of the outgoing (anti)quark that fragments into the Λ, and to obtain a non-zero twist-two spin asymmetry. At higher energies, such as at LEP, even *no* beam polarization is required since the parity-violating $q\bar{q}Z$ coupling automatically generates a net polarization of the quarks. Here, ALEPH [10], DELPHI [11], and OPAL [12] have recently reported first results for the polarization of Λ's produced on the Z-resonance.

Realistic models for the $\Delta D_f^\Lambda(z,Q^2)$ are also of particular relevance for reliable estimates of production rates and spin transfer asymmetries at present and future dedicated spin experiments. Here the $\Delta D_f^\Lambda(z,Q^2)$ can be probed in SIDIS or photoproduction in the current fragmentation region, $lp \to l'\Lambda X$, where either a longitudinally polarized lepton beam or a polarized nucleon target would be required. Such measurements can be carried out at HERMES [13] and are planned by the COMPASS [14] collaboration. After the scheduled upgrade of the HERA electron ring with spin rotators in front of the H1 and ZEUS experiments, longitudinally polarized electrons will be also available for high-energy ep collisions, and similar measurements with polarized Λ's in the final state could be performed here. Furthermore, having also a polarized *proton* beam available at HERA

[15] would allow the measurement of various different twist-2 asymmetries, depending on whether the e and/or the p beam and/or the Λ are polarized, i.e., $\vec{e}p \to \vec{\Lambda}X$, $e\vec{p} \to \vec{\Lambda}X$, and $\vec{e}\vec{p} \to \Lambda X$ (as usual, an arrow denotes a polarized particle).

So far estimates for future Λ experiments have relied on simple models [16] or on Monte-Carlo simulations tuned with several parameters and parametrizations of scale-*in*dependent spin-transfer coefficients C_f^Λ which link longitudinally polarized and unpolarized fragmentation functions via [17]

$$\Delta D_f^\Lambda(z) = C_f^\Lambda(z) D_f^\Lambda(z) \quad . \tag{3}$$

Different phenomenological models for the C_f^Λ exist. A first one is based on the naive non-relativistic quark model where only s-quarks can contribute to the fragmentation processes that eventually yield a polarized Λ. Another approach goes back to estimates by Burkardt and Jaffe [8, 18] for a fictitious DIS structure function g_1^Λ of the Λ, for which sizeable negative contributions from u and d quarks are predicted by analogy with the breaking of the Gourdin-Ellis-Jaffe sum rule [7] for the proton's g_1^p. It is then assumed that such features also carry over to the "time-like" case [18] (see also [17]). Of course, relations like (3) cannot in general hold true in QCD. Due to the different Q^2-evolutions of ΔD_f^Λ and D_f^Λ, it cannot be correct to assume scale independence of the C_f^Λ in (3), and therefore one has to specify a scale at which one implements such an ansatz.

It is the main purpose of this paper to address the issue of fragmentation into polarized Λ's in a detailed QCD analysis. Here it will be possible for us to work even at next-to-leading order (NLO) accuracy, as the required spin-dependent "time-like" two-loop evolution kernels were derived recently [19]. For the first time, we will provide some realistic sets of unpolarized and polarized fragmentation functions for Λ baryons. A useful restrictive constraint when constructing models for the ΔD_f^Λ is provided by the positivity condition (similarly to the "space-like" case), i.e.

$$\left|\Delta D_f^\Lambda(z, Q^2)\right| \leq D_f^\Lambda(z, Q^2) \quad , \tag{4}$$

with the $D_f^\Lambda(z, Q^2)$ taken from the unpolarized analysis. As the available sparse data from LEP are by far not sufficient to completely fix the $\Delta D_f^\Lambda(z, Q^2)$, we will propose

several different sets of polarized fragmentation functions, all compatible with the LEP data. Some of the sets will be based on the ideas outlined in the previous paragraph. Our various proposed ΔD_f^Λ are particularly suited for estimating the physics potential of future experiments to determine the polarized fragmentation functions more precisely. We hence present detailed predictions for future SIDIS measurements at HERMES and the HERA collider. In this context we also provide the necessary framework to calculate helicity transfer cross sections in SIDIS at NLO.

The remainder of the paper is organized as follows: in the next Section we develop the formalism for unpolarized SIA and discuss in detail our analysis of leading order (LO) and NLO Λ fragmentation functions. In Section 3 we turn to the case of longitudinally polarized Λ production and present our different conceivable scenarios for the $\Delta D_f^\Lambda(z, Q^2)$. In Section 4 we compare our unpolarized distributions with recent Λ production data in SIDIS and study the potential of present (HERMES) and future (HERA) spin physics experiments to discriminate between the different proposed sets of polarized fragmentation functions. Finally our results are summarized in Section 5. The Appendices collect the required unpolarized and polarized NLO coefficient functions for SIA and SIDIS.

2 Unpolarized Λ Fragmentation Functions

In the last few years several experiments [2, 3] have reported measurements of the unpolarized cross section for the production of Λ baryons, which allows an extraction of the unpolarized Λ fragmentation functions required for constructing the polarization asymmetries and as reference distributions in the positivity constraint (4). We emphasize at this point that the wide range of c.m.s. energies covered by the data [2, 3] ($14 \leq \sqrt{s} \leq 91.2$ GeV) makes a detailed QCD analysis that includes the Q^2-evolution of the fragmentation functions mandatory.

The cross section for the inclusive production of a hadron H with energy E_H in SIA at a c.m.s. energy $\sqrt{s}$, integrated over the production angle, can be written in the following

way [20, 21]:

$$\frac{1}{\sigma_{tot}}\frac{d\sigma^H}{dx_E} = \frac{1}{\sum_q \hat{e}_q^2}\left[2\,F_1^H(x_E,Q^2) + F_L^H(x_E,Q^2)\right] \ , \tag{5}$$

where $x_E = 2p_H\cdot q/Q^2 = 2E_H/\sqrt{s}$ (q being the momentum of the intermediate γ or Z boson, $q^2 = Q^2 = s$) and

$$\sigma_{tot} = \sum_q \hat{e}_q^2\,\frac{4\pi\alpha^2(Q^2)}{s}\left[1+\frac{\alpha_s(Q^2)}{\pi}\right] \tag{6}$$

is the total cross section for $e^+e^- \to \textit{hadrons}$ including its NLO $\mathcal{O}(\alpha_s)$ correction. The sums in (5), (6) run over the n_f active quark flavours q, and the $\hat{e}_q$ are the corresponding appropriate electroweak charges (see Appendix A for details).

To NLO accuracy the unpolarized "time-like" structure functions F_1^H and F_L^H in (5) are given by

$$\begin{aligned} 2\,F_1^H(x_E,Q^2) &= \sum_q \hat{e}_q^2\left\{\left[D_q^H(x_E,Q^2)+D_{\bar{q}}^H(x_E,Q^2)\right]\right. \qquad (7)\\ &\quad \left. +\frac{\alpha_s(Q^2)}{2\pi}\left[C_q^1\otimes(D_q^H+D_{\bar{q}}^H)+C_g^1\otimes D_g^H\right](x_E,Q^2)\right\} \ , \\ F_L^H(x_E,Q^2) &= \frac{\alpha_s(Q^2)}{2\pi}\sum_q \hat{e}_q^2\,\left[C_q^L\otimes(D_q^H+D_{\bar{q}}^H)+C_g^L\otimes D_g^H\right](x_E,Q^2) \ , \qquad (8) \end{aligned}$$

with the convolutions $\otimes$ being defined as usual by

$$(C\otimes D)(x_E,Q^2) = \int_{x_E}^1 \frac{dy}{y}\,C\left(\frac{x_E}{y}\right)D(y,Q^2) \ . \tag{9}$$

The relevant NLO coefficient functions $C_{q,g}^{1,L}$ [20, 21] can also be found in Appendix A.

To determine the Q^2-evolution of the D_f^H in Eqs. (7), (8) it is as usual convenient to decompose them into flavor singlet and non-singlet pieces by introducing the densities $D_{q,\pm}^H$ and the vector

$$\vec{D}^H \equiv \begin{pmatrix} D_\Sigma^H \\ D_g^H \end{pmatrix} \ , \tag{10}$$

where

$$D_{q,\pm}^H \equiv D_q^H \pm D_{\bar{q}}^H \quad , \quad D_\Sigma^H \equiv \sum_q (D_q^H + D_{\bar{q}}^H) \ . \tag{11}$$

One then has the following non-singlet evolution equations ($q, \tilde{q}$ being two different flavors):

$$\frac{d}{d\ln Q^2}(D^H_{q,+} - D^H_{\tilde{q},+})(z,Q^2) = \left[P^{(T)}_{qq,+} \otimes (D^H_{q,+} - D^H_{\tilde{q},+})\right](z,Q^2)\,, \tag{12}$$

$$\frac{d}{d\ln Q^2} D^H_{q,-}(z,Q^2) = \left[P^{(T)}_{qq,-} \otimes D^H_{q,-}\right](z,Q^2)\ . \tag{13}$$

The two evolution kernels $P^{(T)}_{qq,\pm}(z,\alpha_s(Q^2))$ become different beyond LO as a result of the presence of transitions between quarks and antiquarks. The singlet evolution equation reads

$$\frac{d}{d\ln Q^2}\vec{D}^H(z,Q^2) = \left[\hat{P}^{(T)} \otimes \vec{D}^H\right](z,Q^2)\quad , \tag{14}$$

where we write the singlet evolution matrix $\hat{P}^{(T)}$ as:

$$\hat{P}^{(T)} \equiv \begin{pmatrix} P^{(T)}_{qq} & 2n_f P^{(T)}_{gq} \\ \frac{1}{2n_f} P^{(T)}_{qg} & P^{(T)}_{gg} \end{pmatrix}\ . \tag{15}$$

To NLO, all splitting functions [22, 23] in (12)-(15) have the perturbative expansion

$$P^{(T)}_{ij}(z,\alpha_s) = \left(\frac{\alpha_s}{2\pi}\right) P^{(T),(0)}_{ij}(z) + \left(\frac{\alpha_s}{2\pi}\right)^2 P^{(T),(1)}_{ij}(z)\ . \tag{16}$$

It should be noted that the evolution equations can be straightforwardly solved analytically in Mellin-n space along the lines as, e.g., described in [21]. The desired $D^H_f(z,Q^2)$ are then obtained by a standard numerical Mellin-inversion. Needless to mention that the corresponding LO expressions are entailed in Eqs. (6)-(8) by simply dropping all $\mathcal{O}(\alpha_s)$ contributions and by evolving the $D^H_f(z,Q^2)$ in LO.

In our numerical analysis we cannot include data with $x_E < 0.1$, for two reasons: first of all, for small x_E, finite-mass corrections to Eq. (5) proportional to $4M^2_\Lambda/sx^2_E$ become more and more important, but are not accounted for in the calculation. There is also a more severe limitation set by the evolution equations outlined above: the NLO "time-like" splitting functions $P^{(T),(1)}_{gq}(z)$ and $P^{(T),(1)}_{gg}(z)$ in (15) turn out be much more singular than their corresponding "space-like" counterparts as $z \to 0$. While the leading small-x terms in the "space-like" case are proportional to $1/x$,

$$\lim_{x\to 0} P^{(S)}_{gq}(x) = \frac{\alpha_s}{2\pi}\left(\frac{2C_F}{x} + \frac{\alpha_s}{2\pi}\frac{9C_FC_A - 40C_FT_f}{9x}\right)\,, \tag{17}$$

$$\lim_{x\to 0} P^{(S)}_{gg}(x) = \frac{\alpha_s}{2\pi}\left(\frac{2C_A}{x} + \frac{\alpha_s}{2\pi}\frac{12C_FT_f - 46C_AT_f}{9x}\right)\,, \tag{18}$$

the "time-like" splitting functions show an even stronger negative behaviour for $z \to 0$ due to the dominant large logarithmic piece $\simeq \ln^2 z/z$ in the NLO part,

$$\lim_{z\to 0} P_{gq}^{(T)}(z) = \frac{\alpha_s}{2\pi}\left(\frac{2C_F}{z} - \frac{\alpha_s}{2\pi}\frac{4C_F C_A}{z}\ln^2 z\right) , \tag{19}$$

$$\lim_{z\to 0} P_{gg}^{(T)}(z) = \frac{\alpha_s}{2\pi}\left(\frac{2C_A}{z} - \frac{\alpha_s}{2\pi}\frac{4C_A^2}{z}\ln^2 z\right) \tag{20}$$

(see for example [24]), with the usual QCD colour factors $C_A = 3$, $C_F = 4/3$, and $T_f = T_R n_f = n_f/2$. This singular behaviour of the "time-like" splitting functions is even so strong that it may ultimately lead to *negative* NLO fragmentation functions in the course of the Q^2-evolution and hence to unacceptable *negative* cross sections at some value $x_E \ll 1$, even if the evolution starts with positive distributions at the initial scale. Clearly, the description of fragmentation processes by perturbative QCD without resummation of small-z logarithms breaks down for values of x_E where this happens, and in order to avoid these severe problems we include as usual (see, e.g., [1]) only data with $x_E > 0.1$ in our analysis[1].

As pointed out in [8], the QCD formalism is strictly speaking only applicable to strongly produced Λ's. A certain fraction of the data [2, 3] will, however, consist of secondary Λ's resulting from $e^+e^- \to \Sigma^0 X$ with the subsequent decay $\Sigma^0 \to \Lambda\gamma$, not to be included in the fragmentation functions [8]. For simplicity, we will ignore this problem and (successfully) attempt to describe the full data samples by fragmentation functions that are evolved according to the QCD Q^2-evolution equations.

Unless stated otherwise, we will refer to both Λ^0 and $\bar{\Lambda}^0$, which are not usually distinguished in present e^+e^- experiments [2, 3], as simply "Λ". As a result, the obtained fragmentation functions always correspond to the sum

$$D_f^{\Lambda}(x_E, Q^2) \equiv D_f^{\Lambda^0}(x_E, Q^2) + D_f^{\bar{\Lambda}^0}(x_E, Q^2) \quad . \tag{21}$$

This also considerably simplifies the analysis, since no distinction between "favoured" and "unfavoured" distributions is required. Since no precise SIDIS data are available yet, it is not possible to obtain individual distributions for all the light flavours separately, and

[1] We do not include data either that have been averaged experimentally over a large bin of x_E.

hence some sensible assumptions concerning them have to be made. Employing naive quark model $SU_f(3)$ arguments and neglecting any mass differences between the u, d, and s quarks, we *assume*[2] that all the light flavours fragment equally into Λ, i.e.

$$D_u^\Lambda = D_d^\Lambda = D_s^\Lambda = D_{\bar{u}}^\Lambda = D_{\bar{d}}^\Lambda = D_{\bar{s}}^\Lambda \equiv D_q^\Lambda \quad . \tag{22}$$

Needless to say that the q and $\bar{q}$ fragmentation functions in (22) are equal due to Eq. (21).

At variance with the usual DIS case, *dis*continuous heavy quark (HQ) fragmentation functions should be included at each heavy flavour threshold (see also [1]). Anyway, the inclusion of the HQ contributions essentially only leads to a change in the normalization of the light quark densities, which would just be larger if the HQ ones were not present. In our analysis we start the evolution of the HQ contributions at the mass of the corresponding HQ, but the precise value for this is anyhow irrelevant since all the data are in a region of $s > m_h^2$ $(h = c, b)$.

For our analysis, we choose to work in the framework of the "radiative parton model" which is characterized by a rather low starting scale μ for the Q^2-evolutions. The "radiative parton model" has proven phenomenologically successful in the "space-like" case for both unpolarized [25] and polarized [26] parton densities, and also in the "time-like" situation for photon fragmentation functions [23, 27].

At the initial scale ($\mu_{LO}^2 = 0.23\,\mathrm{GeV}^2$, $\mu_{NLO}^2 = 0.34\,\mathrm{GeV}^2$) we choose the following simple ansatz:

$$D_f^\Lambda(z, \mu^2) = N_f\, z^{\alpha_f} (1 - z)^{\beta_f} \ , \tag{23}$$

where $f = q, c, b, g$ and, as stated, in the case of heavy quarks $\mu^2 = m_h^2$. Utilizing Eq. (22) and assuming for simplicity that $N_c = N_b = N_q$, a total of 10 free parameters remains to be fixed from a fit to the available 103 data points [2, 3] (after applying the x_E cut mentioned above). The total χ^2 values are 103.55 and 104.29 in NLO and LO, respectively, and the optimal parameters in (23) can be found in Table 1. It should be noted that by

[2]Fits allowed to be more general do not seem to improve the final $\chi^2/d.o.f.$

Parameter	LO	NLO ($\overline{\text{MS}}$)
N_q	0.63	0.55
α_q	0.23	0.22
β_q	1.83	2.16
N_g	0.91	2.23
α_g	1.36	1.86
β_g	3.14	3.48
α_c	-0.41	-0.35
β_c	5.66	6.06
α_b	-0.29	-0.32
β_b	5.01	5.45

Table 1: Optimal parameters for the unpolarized fragmentation functions in Eq. (23).

taking into account an additional 4% normalization uncertainty for the LEP data [2], χ^2 can be further reduced but without any noticeable changes in the distributions.

A comparison of our LO and NLO results with the data is presented in Fig. 1, where all the existing data [2, 3] have been converted[3] to the "format" of Eq.(5). One should note that the LO and NLO results are almost indistinguishable, demonstrating the perturbative stability of the process considered. Furthermore, there is an excellent agreement between the predictions of our fits and the data even in the region of "small" x_E which has not been included in our analysis.

Fig. 2 shows our LO and NLO fragmentation functions as specified in Eq. (23) and Table 1, evolved to $Q^2 = 100$ and 10^4 GeV^2. As can be seen, the heavy quark fragmentation functions turn out to be comparable to the light quark ones for small z, whereas they are suppressed for $z \gtrsim 0.3$. It should be also noted that our c and b fragmentation functions are also in agreement with recent results from SLD [3] for the c/uds and b/uds

[3]The available data sets [2, 3] are presented in terms of three different variables: x_E, x_p, and ξ. These variables are simply related to each other by $x_p = \beta x_E$ with $\beta = \sqrt{1 - m_H^2/E_H^2}$, and $\xi = \ln(1/x_p)$.

ratios of Λ production rates in flavour-tagged Z decays.

In Fig. 3 we show our fragmentation functions for light quarks and gluons as functions of Q^2 for several fixed values of z. One can observe the importance of the QCD evolution of the fragmentation functions which we will use for making predictions for SIDIS at Q^2 values much lower than the ones at which the fragmentation functions were extracted.

Finally, we investigate the contribution of our Λ (more precisely $\Lambda + \bar{\Lambda}$, see Eq. (21)) fragmentation functions $D_f^\Lambda(z, Q^2)$ to the momentum sum rule

$$\sum_H \int_0^1 dz z D_f^H(z, Q^2) = 1 \quad . \tag{24}$$

Eq. (24) expresses the conservation of the momentum of the fragmenting parton f in the fragmentation process, i.e. each parton f will fragment with 100% probability into some hadron H. Of course the sum rule (24) should be dominated, even almost saturated, by the fragmentation into the lightest hadrons such as π and K mesons. Hence the contribution to (24) due to D_f^Λ is expected to be rather small. Indeed we find that in LO and NLO the contribution of our light quark (gluon) $\Lambda + \bar{\Lambda}$ fragmentation functions to the momentum sum rule (24) only amounts to about $2 - 3\%$ $(1 - 2\%)$.

3 Polarized Fragmentation Functions

Having obtained a reliable set of unpolarized fragmentation functions we now turn to the polarized case where unfortunately only scarce and far less precise data are available. In fact, no data at all have been obtained so far using polarized beams. The only available information comes from *un*polarized LEP measurements [10-12] profitting from the parity-violating electroweak $q\bar{q}Z$ coupling.

For such measurements, done *at* the mass of the Z boson (Z-resonance), the cross section for the production of polarized hadrons can be written as [8, 28]

$$\frac{d\Delta\sigma^H}{d\Omega dx_E} = 3\frac{\alpha^2(Q^2)}{2s}\Big[g_3^H(x_E, Q^2)(1 + \cos^2\theta) - g_1^H(x_E, Q^2)\cos\theta + g_L^H(x_E, Q^2)(1 - \cos^2\theta)\Big] \, . \tag{25}$$

If, as for the quoted experimental results [10-12], the cross section is integrated over the production angle θ, the anyway small, charge suppressed contribution from g_1^H drops out. One can then define the asymmetry

$$A^H = \frac{g_3^H + g_L^H/2}{F_1^H + F_L^H/2} \tag{26}$$

which corresponds to the "Λ-polarization" observable measured at LEP. The polarized structure functions g_1^H, g_3^H and g_L^H in (25) and (26) are given in NLO by the following expressions:

$$\begin{aligned} g_1^H(x_E,Q^2) &= \sum_q g_q' \Big\{ \left[\Delta D_q^H(x_E,Q^2) + \Delta D_{\bar{q}}^H(x_E,Q^2)\right] \\ &\quad + \frac{\alpha_s(Q^2)}{2\pi} \left[\Delta C_q^1 \otimes (\Delta D_q^H + \Delta D_{\bar{q}}^H) + \Delta C_g^1 \otimes \Delta D_g^H\right](x_E,Q^2) \Big\} \end{aligned} \tag{27}$$

$$\begin{aligned} g_3^H(x_E,Q^2) &= \sum_q g_q \Big\{ \left[\Delta D_q^H(x_E,Q^2) - \Delta D_{\bar{q}}^H(x_E,Q^2)\right] \\ &\quad + \frac{\alpha_s(Q^2)}{2\pi} \left[\Delta C_q^3 \otimes (\Delta D_q^H - \Delta D_{\bar{q}}^H)\right](x_E,Q^2) \Big\} \end{aligned} \tag{28}$$

$$g_L^H(x_E,Q^2) = \frac{\alpha_s(Q^2)}{2\pi} \sum_q g_q \left[\Delta C_q^L \otimes (\Delta D_q^H - \Delta D_{\bar{q}}^H)\right](x_E,Q^2)\,, \tag{29}$$

with the convolutions as already defined in (9). The appropriate effective charges g_q and g_q' as well as the required spin-dependent $\overline{\rm MS}$ coefficients $\Delta C_{q,g}^{1,3,L}$ in (27)-(29) can be found in Appendix B.

Note that both g_3^H and g_L^H in (28), (29) are *non-singlet* structure functions, and hence only the *valence* part of the polarized fragmentation functions can be obtained from the available LEP data [10-12]. In addition the Λ^0's and $\bar{\Lambda}^0$'s give contributions of opposite signs to the measured polarization and thus to $g_{3,L}^{\Lambda}$. Unfortunately, it is clear that the available LEP data [10-12], all obtained *on* the Z-resonance, cannot even sufficiently constrain the valence distributions for all the flavours, so some assumptions have to be made here. Obviously, even further assumptions are needed for the polarized gluon and sea fragmentation functions in order to have a complete set of fragmentation functions suitable for predictions for other processes, in particular for SIDIS (see Section 4).

In the present analysis the heavy flavour contributions to polarized Λ production are neglected, and u and d fragmentation functions are taken to be equal. Furthermore,

polarized "unfavoured" distributions, i.e., $\Delta D_{\bar{u}}^{\Lambda^0} = \Delta D_u^{\bar{\Lambda}^0}$, etc., and the gluon fragmentation function ΔD_g^{Λ} are *assumed* to be negligible at the initial scale μ, an assumption which of course deserves a further scrutiny (we will discuss the impact of choosing a different boundary condition for the gluon fragmentation function later). The remaining spin-dependent quark fragmentation functions are then related to the corresponding unpolarized ones taken from Section 2 in the following simple way

$$\Delta D_s^{\Lambda}(z,\mu^2) = z^{\alpha} D_s^{\Lambda}(z,\mu^2) \;\; , \;\; \Delta D_u^{\Lambda}(z,\mu^2) = \Delta D_d^{\Lambda}(z,\mu^2) = N_u \, \Delta D_s^{\Lambda}(z,\mu^2) \;\; . \tag{30}$$

They are subject to the positivity constraints (4), which simply imply $\alpha > 0$ and $|N_u| \leq 1$. These input distributions are then evolved to higher Q^2 via the appropriate Altarelli-Parisi equations which are completely similar to the ones presented in Eqs. (10)-(16), with just all unpolarized quantities (like, for instance, $\hat{P}^{(T)}$) replaced by their appropriate polarized counterparts. For the NLO evolution one has to use for this purpose the spin-dependent "time-like" two-loop splitting functions as derived in [19] in the $\overline{\rm MS}$ scheme. Due to the rather limited amount of available data it does not appear reasonable for the time being to introduce more free parameters than the two in Eq. (30).

Within this framework we try three different scenarios for the polarized fragmentation functions at our low initial scale μ, to cover a rather wide range of plausible models:

Scenario 1 corresponds to the expectations from the non-relativistic naive quark model where only s-quarks can contribute to the fragmentation processes that eventually yield a polarized Λ, even if the Λ is formed via the decay of a heavier hyperon. We hence have $N_u = 0$ in (30) for this case.

Scenario 2 is based on estimates by Burkardt and Jaffe [8, 18] for the "space-like" DIS structure function g_1^{Λ} of the Λ, predicting sizeable negative contributions from u and d quarks to g_1^{Λ} by analogy with the breaking of the Gourdin-Ellis-Jaffe sum rule [7] for the proton's g_1^p. Assuming that such features also carry over to the "time-like" case [18], we simply impose $N_u = -0.20$ (see also [17]).

Scenario 3: All the polarized fragmentation functions are assumed to be equal here, i.e. $N_u = 1$, contrary to the expectation of the non-relativistic quark model used in

scen. 1. This rather "extreme" scenario might be realistic if, for instance, there are sizeable contributions to polarized Λ production from decays of heavier hyperons who have inherited the polarization of originally produced u and d quarks.

Parameter	LO			NLO ($\overline{\text{MS}}$)		
	scen. 1	scen. 2	scen. 3	scen. 1	scen. 2	scen. 3
N_u	0	-0.2	1.0	0	-0.2	1.0
α	0.62	0.27	1.66	0.44	0.13	1.33

Table 2: Resulting optimal LO and NLO fit parameters as introduced in (30) for the three different scenarios described in the text.

Our results for the asymmetry A^Λ in (26) within the three different scenarios are compared to the available LEP data [10-12] in Fig. 4. The optimal parameters in (30) for the three models can be found in Table 2. As can be seen, the best agreement with the data is obtained within the (naively) most unlikely scen. 3. The differences occur mainly in the region of large x_E, where scen. 1 and 2 cannot fully account for the rather large observed polarization. It turns out that this is a consequence of the assumed $SU(3)_f$ symmetry for the *un*polarized fragmentation functions, and of the positivity constraints (4): for instance, $SU(3)_f$ symmetry of the D_q^Λ implies in the case of scen. 1 that the asymmetry at large x_E behaves asymptotically roughly like $-\Delta D_s^\Lambda/3D_s^\Lambda$. Thus, even when saturating the positivity constraint (4) at around $x_E = 0.5$ it is not possible to obtain a polarization as large as the one required by the ALEPH and OPAL data [10, 12]. We note that the assumed $SU(3)_f$ symmetry for the unpolarized fragmentation functions could of course be broken. It is clear at this point that further information on the polarized *and* the unpolarized Λ fragmentation functions is needed, which could be provided by future precise SIDIS measurements.

Finally, in Fig. 5 we show the LO and NLO partonic fragmentation asymmetries for each flavour distribution separately, i.e. $A_f \equiv \Delta D_f^\Lambda / D_f^\Lambda$. A positive polarized gluon fragmentation function has built up in the Q^2-evolution in spite of the vanishing input at μ^2. In order to analyze the effect of imposing a different boundary condition for the polarized gluon fragmentation function, we include in Fig. 5 also the results of a

LO fit similar to the one performed within scenario 1, but now using the maximally allowed polarized gluon input $\Delta D_g(\mu^2) = D_g(\mu^2)$ instead of $\Delta D_g(\mu^2) = 0$. Besides the expected result of having now a larger gluon polarization at $Q^2 = 10$ GeV^2, an important enhancement of the u and d distributions (which are practically vanishing in the original scenario 1) can be observed, which is due to the perturbative generation of sea by polarized gluons in the course of the evolution. In fact, at small values of z, the u and d distributions become even larger than the ones of scenario 3. Obviously, only different combined further measurements, like in e^+e^- annihilation and SIDIS with polarized beams, will be capable of determining the gluon (and also the sea) fragmentation function more precisely.

4 Λ Production in SIDIS

Equipped with various sets of polarized fragmentation functions, let us now turn to the SIDIS process $eN \to e'HX$ which should be very well suited to give further information on fragmentation functions. In this case, the cross section is proportional to a combination of both the parton distributions of the nucleon N and the fragmentation functions for the hadron H. The latter thus automatically appear in a constellation different from the one probed in e^+e^- annihilation.

In the particular case where both nucleon and hadron are unpolarized, the cross section can be written in a way similar to the fully inclusive DIS case [20, 21, 30]:

$$\frac{d\sigma^H}{dx\,dy\,dz_H} = \frac{2\,\pi\alpha^2}{Q^2}\left[\frac{(1+(1-y)^2)}{y}2\,F_1^{N/H}(x,z_H,Q^2) + \frac{2(1-y)}{y}F_L^{N/H}(x,z_H,Q^2)\right] \quad , \tag{31}$$

with x and y denoting the usual DIS scaling variables ($Q^2 = sxy$), and where [20, 21] $z_H \equiv p_H \cdot p_N / p_N \cdot q$ with an obvious notation of the four-momenta, and with $-q^2 \equiv Q^2$. Strictly speaking, Eq. (31) and the variable z_H only apply to hadron production in the current fragmentation region. In this work, we will effectively eliminate the target fragmentation region by implementing a cut $x_F > 0$ on the Feynman-variable representing the fractional longitudinal c.m.s. momentum. Target fragmentation could be accounted

for by transforming to the variable [29-32]

$$z_H \to z \equiv \frac{E_H}{E_N(1-x)} \ , \tag{32}$$

the energies E_H, E_N defined in the c.m.s. frame of the nucleon and the virtual photon, and by introducing the so-called "fracture functions" [29]. The inclusion of the latter is beyond the scope of this analysis [33] and anyway not relevant numerically due to the cut on x_F. The variable z in (32) is also better suited for dealing with corrections due to the finite target mass M_H. As will be demonstrated below, it is not always justified to neglect these. Our predictions for Λ production in SIDIS will therefore be made using the variable z. The NLO corrections to $F_1^{N/H}$ and $F_L^{N/H}$ in (31) can, however, be expressed much more conveniently in terms of z_H (see Appendix C). The transformation from z_H to z is straightforward [29-32].

The structure functions $F_1^{N/H}$ and $F_L^{N/H}$ in (31) are given at NLO by

$$\begin{aligned} 2\,F_1^{N/H}(x,z_H,Q^2) &= \sum_{q,\overline{q}} e_q^2 \Bigg\{ q(x,Q^2) D_q^H(z_H,Q^2) + \frac{\alpha_s(Q^2)}{2\pi} \Big[q \otimes C_{qq}^1 \otimes D_q^H \\ &+ q \otimes C_{gq}^1 \otimes D_g^H + g \otimes C_{qg}^1 \otimes D_q^H \Big](x,z_H,Q^2) \Bigg\} \qquad (33) \\ F_L^{N/H}(x,z_H,Q^2) &= \frac{\alpha_s(Q^2)}{2\pi} \sum_{q,\overline{q}} e_q^2 \Big[q \otimes C_{qq}^L \otimes D_q^H \\ &+ q \otimes C_{gq}^L \otimes D_g^H + g \otimes C_{qg}^L \otimes D_q^H \Big](x,z_H,Q^2) \ , \qquad (34) \end{aligned}$$

with the NLO coefficient functions $C_{ij}^{1,L}$ [20, 21, 30] collected in Appendix C.

As already mentioned in the Introduction, three other possible cross sections can be defined when the polarization of the lepton, the initial nucleon and the hadron are taken into account. If both nucleon and hadron are polarized and the lepton is unpolarized, the expression is similar to Eqs. (31)-(34) above with, however, the unpolarized parton distributions *and* the fragmentation functions to be replaced by their polarized counterparts. Obviously, one also has to adapt the coefficient functions to this case: $C_{ij}^{1,L} \to \Delta C_{ij}^{1,L,NH}$. The relevant expressions can again be found in Appendix C. In the case that the lepton and either the nucleon *or* the hadron are polarized, the expression for the cross section is

given as in the fully inclusive case by a single structure function $g_1^{N/H}(x, z_H, Q^2)$:

$$\frac{d\Delta\sigma^H}{dx\,dy\,dz_H} = \frac{4\pi\alpha^2}{Q^2}(2-y)\,g_1^{N/H}(x, z_H, Q^2)\;. \tag{35}$$

To NLO, $g_1^{N/H}$ can be written as [31, 32, 34]

$$\begin{aligned} 2\,g_1^{N/H}(x, z_H, Q^2) &= \sum_{q,\bar{q}} e_q^2 \Big\{ (\Delta)q(x,Q^2)(\Delta)D_q^H(z_H,Q^2) \\ &+ \frac{\alpha_s(Q^2)}{2\pi}\Big[(\Delta)q \otimes \Delta C_{qq}^i \otimes (\Delta)D_q^H + (\Delta)q \otimes \Delta C_{gq}^i \otimes (\Delta)D_g^H \\ &+ (\Delta)g \otimes \Delta C_{qg}^i \otimes (\Delta)D_q^H\Big](x, z_H, Q^2)\Big\}\;, \end{aligned} \tag{36}$$

the position of the Δ and the index $i = N, H$ depending on which particle (N or H) is polarized. Again, all NLO $\overline{\rm MS}$ coefficient functions ΔC_{jk}^i are collected in Appendix C.

Let us first turn to the entirely unpolarized case as defined in Eq. (31), which could prove invaluable for obtaining a flavour separation of fragmentation functions not provided by the SIA data. Unfortunately, only three measurements of this cross section exist up to now [4], with still rather large experimental uncertainties. It is nevertheless worth comparing our predictions to the available data in order to test our proposed fragmentation functions in a process other than SIA.

The original experimental results [4] are compiled in Fig. 6a, where the data are plotted in terms of the Feynman variable x_F. As can be observed, differences between results at different values of the $\gamma^* p$ c.m.s. energy W are much larger than expected from the scale dependence, especially at small x_F. The reason for this is simple and corresponds to the fact that the variable x_F is not the scaling variable of this process, i.e. the argument of the fragmentation functions in Eq. (31). As already mentioned, Eq. (31) should be expressed in terms of z in (32) [30]. At LO, z coincides with x_F and also with the variable z_H introduced in (31) [20, 21], *if* the mass of the Λ is neglected. However, it again turns out that, as in the case of SIA, finite-mass effects introduced by the function $\beta = \sqrt{1 - 4M_\Lambda^2/(zW)^2}$ become relevant at small z for the low-W experiments. The other two variables are at LO given in terms of β and z by $x_F = \beta\, z$ and $z_H = (1+\beta)/2\, z$. In Fig. 6b we show the same data as in Fig. 6a, but converted to the variable z, where now a much better agreement between different experimental data and also with our

LO predictions plotted for three different typical scales can be observed. It should be noticed that the H1 data [4] were obtained with an integrated luminosity of only 1.3 pb^{-1}, so a more dedicated measurement in the future will be very helpful in determining the unpolarized Λ fragmentation functions more precisely.

The most interesting observable with respect to the determination of the *polarized* Λ fragmentation functions is of course the asymmetry for the production of polarized Λ's from an *un*polarized proton, defined by $A^\Lambda \equiv g_1^{p/\Lambda}/F_1^{p/\Lambda}$ [18] with $g_1^{p/\Lambda}$ given by (36) with $i = H$. In Fig. 7a, we show our LO and NLO predictions for HERA with polarized electrons and *un*polarized protons using the GRV parton distributions [25], integrated over the measurable range $0.1 \leq z \leq 1$. The values for Q^2 that correspond to each x-bin have been chosen as in [35]. Good perturbative stability of the process is found. As can be seen, the results obtained using the three distinct scenarios for polarized fragmentation functions turn out to be completely different. Since the asymmetry at small x is determined by the proton's sea quarks, its behaviour can be easily understood: in scen. 1 only s quarks fragment into polarized Λ's, giving an asymmetry which is positive but about three times smaller than the one of scen. 3 where all the flavours contribute. In the case of scen. 2 the positive contribution from the s-quark fragmentation is cancelled by a negative one from u and d, resulting in an almost vanishing asymmetry. The interpretation is similar for the region of large x, where only the contribution involving u_v is sizeable and the asymmetry asymptotically goes to $\int dz \Delta D_u^\Lambda / \int dz D_u^\Lambda$ for each scenario.

We have included in Fig. 7a also the expected statistical errors for HERA, computed assuming an integrated luminosity of 500 pb^{-1} and a realistic value of $\epsilon = 0.1$ for the efficiency of Λ detection [36]. Comparing the asymmetries and the error bars in Fig. 7a one concludes that a measurement of A^Λ at small x would allow a discrimination between different conceivable scenarios for polarized fragmentation functions. Fig. 7b shows our results vs. z for fixed $x = 5.6 \cdot 10^{-4}$. Again, very different asymmetries are found for the three scenarios. In this plot we also include the expectation from scenario 1 with a maximal gluon polarization (see Sec. 3) which, as expected, predicts a larger asymmetry at small z (comparable to the one of scenario 3) mainly due to the contribution of the

radiated sea.

In Fig. 8 we show the same observable for the case of HERMES, where the Q^2 values were chosen as for the inclusive DIS measurements by HERMES [37]. This fixed target experiment analyses a different kinematical region of both larger x and z ($z > 0.3$) and hence could provide complementary information. As can be seen by comparing Figs. 7b and 8b, the asymmetry for scenario 3 shows a similar behaviour for both experiments, which is expected as all the fragmentation functions are equal and the parton distributions cancel in the ratio (at LO). However, the asymmetries predicted by scenarios 1 and 2 change quite a bit when going from HERA collider to fixed target energies due to the fact that for the values of x probed at HERMES the contributions from the valence distributions dominate. Thus more weight is given to the $D^{\Lambda}_{u,d}$ fragmentation functions, and the contributions involving D^{Λ}_{s} are suppressed, in contrast to the situation for the small x-region to be explored by HERA. Again we show in Fig. 8b also the results for scenario 1 with a maximally saturated gluon fragmentation function at the input scale which leads to results hardly different from the standard one since the sea contribution is negligible at large z.

Finally, the particular case of both target and hadron being polarized was originally proposed as a very good way to obtain the Δs distribution [38]. The underlying assumption here was that only the fragmentation function ΔD^{Λ}_{s} is sizeable (as realized, e.g. in our scenario 1), and that therefore the only contribution to the polarized cross section has to be proportional to $\Delta s \Delta D^{\Lambda}_{s}$. In order to analyze the sensitivity of the corresponding asymmetry to Δs, we compute it using the two different GRSV sets of polarized parton densities of the proton [26], which mainly differ in the strange distribution: the so-called "standard" set assumes an unbroken $SU(3)_f$ symmetric sea, whereas in the "valence" scenario the sea is maximally broken and the resulting strange quark density is quite small.

The results for HERA are shown in Fig. 9. Unfortunately – and not unexpectedly – it turns out that the differences in the asymmetry resulting from our different models for polarized Λ fragmentation are far larger than the ones due to employing different

polarized proton strange densities. In addition, a distinction between different Δs would remain elusive even if the spin-dependent Λ fragmentation functions were known to good accuracy, as can be seen from the error bars in Fig. 9 which were obtained using the same parameters as before.

5 Summary and Conclusions

We have performed a detailed QCD analysis of the production of Λ baryons in e^+e^- annihilation and semi-inclusive deep-inelastic scattering.

Working within the framework of the radiative parton model, our starting point has been a fit to unpolarized data for Λ production taken in e^+e^- annihilation, yielding a set of realistic unpolarized fragmentation functions for the Λ. We have then made simple assumptions for the relation between the spin-dependent and the unpolarized Λ fragmentation functions at the input scale for the Q^2-evolution. Taking into account the sparse LEP data on the polarization of $\Lambda's$ produced on the Z-resonance, we were able to set up three distinct "toy scenarios" for the spin-dependent Λ fragmentation functions, to be used for predictions for future experiments. We emphasize that our proposed sets can by no means cover all the allowed possibilities for the polarized fragmentation functions, the main reason being that the LEP data are only sensitive to the valence part of the polarized fragmentation functions. Thus, there are still big uncertainties related to the "unfavoured" quark and gluon fragmentation functions, making further measurements in other processes indispensable.

Under these premises, we have studied Λ production in semi-inclusive deep-inelastic scattering. Existing data for the production of unpolarized Λ's are well described by our fragmentation functions determined from the e^+e^- annihilation data. Turning to spin transfer asymmetries sensitive to the longitudinal polarization of the produced Λ's, we have considered both $\vec{e}p \to \vec{\Lambda}X$ and $e\vec{p} \to \vec{\Lambda}X$ scattering. It turns out that in the first case SIDIS measurements at HERA (with spin-rotators in front of the H1 and ZEUS detectors) and at HERMES should be particularly well suited to yield further information on the

ΔD_f^Λ: differences between the asymmetries obtained when using different sets of ΔD_f^Λ are usually larger than the expected statistical errors. In contrast to this, having a polarized proton target (or beam) does not appear beneficial as far as Λ production is concerned.

A FORTRAN package containing our unpolarized and polarized LO and NLO Λ fragmentation functions can be obtained by electronic mail from Daniel.Deflorian@cern.ch, Marco.Stratmann@durham.ac.uk, or Werner.Vogelsang@cern.ch upon request.

Acknowledgements

The work of one of us (DdF) was partially supported by the World Laboratory.

Appendix A: Unpolarized SIA

The NLO ($\overline{\rm MS}$) coefficients $C_{q,g}^{1,L}$ in (7) and (8) are given by [20, 21]:

$$\begin{aligned} C_q^1(z) &= C_F\left[(1+z^2)\left(\frac{\ln(1-z)}{1-z}\right)_+ - \frac{3}{2}\frac{1}{(1-z)_+}\right. \\ &\quad \left. +2\,\frac{1+z^2}{1-z}\ln z + \frac{3}{2}(1-z) + \left(\frac{2}{3}\pi^2 - \frac{9}{2}\right)\delta(1-z)\right] \qquad \text{(A.1)} \\ C_g^1(z) &= 2\,C_F\left[\frac{1+(1-z)^2}{z}\,\ln\left(z^2(1-z)\right) - 2\,\frac{1-z}{z}\right] \qquad \text{(A.2)} \\ C_q^L(z) &= C_F \qquad \text{(A.3)} \\ C_g^L(z) &= 4\,C_F\,\frac{(1-z)}{z} \qquad \text{(A.4)} \end{aligned}$$

with $C_F = 4/3$. Note that in the expressions for $C_{q,g}^1$ we have taken the factorization scales for the final-state mass singularities to be equal to the hard scale Q of the process, as we did in all our numerical applications. The "+"-prescription is defined as usual by

$$\int_0^1 dz f(z)\,(g(z))_+ \equiv \int_0^1 dz\,[f(z)-f(1)]\,g(z)\ . \qquad \text{(A.5)}$$

The electroweak charges in (5)-(8) are given by

$$\hat{e}_q^2 = e_q^2 - 2e_q\chi_1(Q^2)V_eV_q + \chi_2(Q^2)(1+V_e^2)(1+V_q^2) \qquad \text{(A.6)}$$

where

$$\begin{aligned}\chi_1(s) &= \frac{1}{16\,\sin^2\Theta_W\cos^2\Theta_W}\frac{s\,(s-M_Z^2)}{(s-M_Z^2)^2+\Gamma_Z^2M_Z^2}\\ \chi_2(s) &= \frac{1}{256\,\sin^4\Theta_W\cos^4\Theta_W}\frac{s^2}{(s-M_Z^2)^2+\Gamma_Z^2M_Z^2}\ .\end{aligned}\tag{A.7}$$

Here e_q is the fractional electromagnetic quark charge, and M_Z and Γ_Z are the mass and the decay width of the Z boson, respectively. The other electroweak couplings are given in terms of the Weinberg angle Θ_W by

$$\begin{aligned}V_e &= -1+4\sin^2\Theta_W\\ V_u &= +1-\frac{8}{3}\sin^2\Theta_W\\ V_d &= -1+\frac{4}{3}\sin^2\Theta_W\ .\end{aligned}\tag{A.8}$$

Appendix B: Polarized SIA

The NLO $\overline{\rm MS}$ coefficients $\Delta C_{q,g}^{1,3,L}$ in (27)-(29) read:

$$\Delta C_q^1(z) = C_q^1(z) - C_F\,[1-z]\tag{B.1}$$

$$\Delta C_g^1(z) = 2C_F\Big[(2-z)\,\ln\left(z^2(1-z)\right)-4+3\,z\Big]\tag{B.2}$$

$$\Delta C_q^3(z) = C_q^1(z)\tag{B.3}$$

$$\Delta C_q^L(z) = C_q^L(z)\quad ,\tag{B.4}$$

where the effective charges *on* the Z-resonance are given by [8]

$$g_q = \chi_2(M_Z^2)A_q\,V_q(1+V_e^2)\tag{B.5}$$

$$g_q' = 2\,\chi_2(M_Z^2)V_e(1+V_q^2)\ ,\tag{B.6}$$

where $A_u=-A_d=1$ and V_e, V_q, $\chi_2(s)$ have already been defined in (A.7), (A.8). The structure functions g_3^H and g_L^H in Eqs. (28), (29) are purely non-singlet and therefore do not receive a gluonic correction.

One should note that the NLO quark corrections for the unpolarized case, see Eqs. (A.1) and (A.3), and the ones for the spin-dependent parity violating structure functions

g_3^H and g_L^H in (B.3), (B.4) are identical, which results from identical tensorial structures at the parton level. The expressions for $\Delta C_q^1(z)$ and $\Delta C_g^1(z)$ in the $\overline{\rm MS}$ scheme were already derived in [32, 19]. The difference $\Delta C_q^1(z) - C_q^1(z)$ in (B.1) is independent of the regularization prescription chosen and coincides with the one found in [28] by using off-shell gluons to regularize the collinear singularities.

Appendix C: Unpolarized and Polarized SIDIS Coefficient Functions

Here we list all unpolarized and polarized NLO ($\overline{\rm MS}$) coefficients $(\Delta)C_{\cdots}^{\cdots}$ for SIDIS as introduced in Section 4. To keep the expressions as short as possible it is convenient to define the following abbreviations

$$\begin{aligned}
\tilde{P}_{qq}(\xi) &= \frac{1+\xi^2}{(1-\xi)_+} \quad + \quad \frac{3}{2}\delta(1-\xi) \ , \\
\tilde{P}_{gq}(\xi) &= \frac{1+(1-\xi)^2}{\xi} \quad , \quad \Delta\tilde{P}_{gq}(\xi) = \frac{1-(1-\xi)^2}{\xi} = 2-\xi \ , \\
\tilde{P}_{qg}(\xi) &= \xi^2+(1-\xi)^2 \quad , \quad \Delta\tilde{P}_{qg}(\xi) = \xi^2-(1-\xi)^2 = 2\xi-1 \ , \\
L_1(\xi) &= (1+\xi^2)\left(\frac{\ln(1-\xi)}{1-\xi}\right)_+ \quad , \quad L_2(\xi) = \frac{1+\xi^2}{1-\xi}\ln\xi \ . \qquad \text{(C.1)}
\end{aligned}$$

Note that in what follows we always suppress the argument (x, z) of the coefficient functions. M and M_F denote the factorization scales for initial and final state mass singularities, respectively. Note that for all our numerical calculations we have chosen as usual $M = M_F = Q$. All results presented here are given in the $\overline{\rm MS}$ scheme, and in case of the spin-dependent coefficients ΔC_{qq}^i the additional finite subtractions that are required when using the γ_5 prescription of [39], have been performed along the lines discussed in [40, 19].

Coefficients for $eN \to e'HX$: [21]

$$\begin{aligned}
C_{qq}^1 &= C_F\Bigg[-8\delta(1-x)\delta(1-z) + \\
&\quad \delta(1-x)\left[\tilde{P}_{qq}(z)\ln\frac{Q^2}{M_F^2} + L_1(z) + L_2(z) + (1-z)\right] +
\end{aligned}$$

$$\delta(1-z)\left[\tilde{P}_{qq}(x)\ln\frac{Q^2}{M^2}+L_1(x)-L_2(x)+(1-x)\right]+$$
$$2\frac{1}{(1-x)_+}\frac{1}{(1-z)_+}-\frac{1+z}{(1-x)_+}-\frac{1+x}{(1-z)_+}+2(1+xz)\Bigg] \tag{C.2}$$

$$C^1_{gq} = C_F\Bigg[\tilde{P}_{gq}(z)\left(\delta(1-x)\ln\left(\frac{Q^2}{M_F^2}z(1-z)\right)+\frac{1}{(1-x)_+}\right)+$$
$$z\delta(1-x)+2(1+x-xz)-\frac{1+x}{z}\Bigg] \tag{C.3}$$

$$C^1_{qg} = \frac{1}{2}\Bigg[\delta(1-z)\left[\tilde{P}_{qg}(x)\ln\left(\frac{Q^2}{M^2}\frac{1-x}{x}\right)+2x(1-x)\right]+$$
$$\tilde{P}_{qg}(x)\left\{\frac{1}{(1-z)_+}+\frac{1}{z}-2\right\}\Bigg] \tag{C.4}$$

$$C^L_{qq} = 4C_F xz \tag{C.5}$$

$$C^L_{gq} = 4C_F x(1-z) \tag{C.6}$$

$$C^L_{qg} = 4x(1-x) \tag{C.7}$$

Coefficients for $\vec{e}\vec{N}\to e'HX$:

$$\Delta C^N_{qq} = C^1_{qq}-2C_F(1-x)(1-z) \tag{C.8}$$

$$\Delta C^N_{gq} = C^1_{gq}-2C_F z(1-x) \tag{C.9}$$

$$\Delta C^N_{qg} = \frac{1}{2}\Bigg(\delta(1-z)\left[\Delta\tilde{P}_{qg}(x)\ln\left(\frac{Q^2}{M^2}\frac{1-x}{x}\right)+2(1-x)\right]+$$
$$\Delta\tilde{P}_{qg}(x)\left[\frac{1}{(1-z)_+}+\frac{1}{z}-2\right]\Bigg) \tag{C.10}$$

Coefficients for $\vec{e}N\to e'\vec{H}X$:

$$\Delta C^H_{qq} = \Delta C^N_{qq}+2C_F(1-z)\delta(1-x) \tag{C.11}$$

$$\Delta C^H_{gq} = C_F\Bigg\{\Delta\tilde{P}_{gq}(z)\left[\delta(1-x)\ln\left(\frac{Q^2}{M_F^2}z(1-z)\right)+\frac{1}{(1-x)_+}\right]-$$
$$2(1-z)\delta(1-x)-2(1+x-z)+\frac{1+x}{z}\Bigg\} \tag{C.12}$$

$$\Delta C^H_{qg} = C^1_{qg}-\tilde{P}_{qg}(x)\frac{1-z}{z} \tag{C.13}$$

Coefficients for $e\vec{N}\to e'\vec{H}X$:

$$\Delta C^{1,NH}_{qq} = C^1_{qq}+2C_F(1-z)\delta(1-x) \tag{C.14}$$

$$\Delta C_{qq}^{1,NH} = \Delta C_{qq}^{H} - 2C_F z(1-x) \tag{C.15}$$

$$\Delta C_{qg}^{1,NH} = \Delta C_{qg}^{N} - \Delta\tilde{P}_{qg}(x)\frac{1-z}{z} \tag{C.16}$$

$$\Delta C_{qq}^{L,NH} = C_{qq}^{L} \tag{C.17}$$

$$\Delta C_{gq}^{L,NH} = -4C_F x(1-z) \tag{C.18}$$

$$\Delta C_{qg}^{L,NH} = 0 \quad . \tag{C.19}$$

We note that all our results for the spin-dependent coefficients in (C.8)-(C.19) coincide with the ones presented in [34] and also fully agree with the results of [31, 32] if one carefully disentangles in these papers the contributions from the current and the target fragmentation regions (in the same way our unpolarized results in (C.2)-(C.7) are in agreement with ref. [30]). In addition, one has to account for the slightly different factorization scheme used in ref. [31].

Finally let us show how to deal with the "+" - distributions appearing in the expressions above. The "+" - distribution was already defined in Eq. (A.5) in Appendix A. In practice, however, the lower limit of the integration in (A.5) is different from zero, hence the distributions have to be modified according to [41]:

$$\begin{aligned} \frac{1}{(1-\xi)_+} &= \frac{1}{(1-\xi)_A} + \ln(1-A)\delta(1-\xi) \ , \\ \left(\frac{\ln 1-\xi}{1-\xi}\right)_+ &= \left(\frac{\ln 1-\xi}{1-\xi}\right)_A + \frac{1}{2}\ln^2(1-A)\delta(1-\xi) \ , \end{aligned} \tag{C.20}$$

where $(\,)_A$ is defined as in (A.5) but with the lower integration limit replaced by A. In addition, in the coefficients $(\Delta)C_{qq}^{i}$ listed above also double "+" - distributions appear, which can be defined in analogy with Eq. (A.5) by

$$\int_0^1 dx \int_0^1 dz \frac{f(x,z)}{(1-x)_+(1-z)_+} \equiv \int_0^1 \int_0^1 dxdz \ \frac{f(x,z) - f(1,z) - f(x,1) + f(1,1)}{(1-x)(1-z)} \ . \tag{C.21}$$

Again, in practice the lower integration limits are both different from zero, say, A for the x integration and B for the z integration, and the distribution defined above can be rewritten as

$$\frac{1}{(1-x)_+(1-z)_+} = \frac{1}{(1-x)_A(1-z)_B} + \frac{1}{(1-x)_A}\ln(1-B)\delta(1-z) +$$

$$\frac{1}{(1-z)_B}\ln(1-A)\delta(1-x)+\ln(1-A)\ln(1-B)\delta(1-x)\delta(1-z)\ . \qquad \text{(C.22)}$$

References

[1] J. Binnewies, B.A. Kniehl and G. Kramer, Phys. Rev. **D52**, 4947 (1995).

[2] G. Alexander et al., OPAL collab., Z. Phys. **C73**, 569 (1997);
M. Acciarri et al., L3 collab., Phys. Lett. **B407**, 389 (1997);
For a compilation of the previously published e^+e^- data see: G.D. Lafferty, P.I. Reeves, and M.R. Whalley, J. Phys. **G21**, A1 (1995).

[3] K. Abe et al., SLD collab., SLAC-PUB-7571, paper submitted to the "XVIII International Symposium on Lepton Photon Interactions", 1997, Hamburg, Germany, and to the "International Europhysics Conference on High Energy Physics", 1997, Jerusalem, Israel.

[4] S. Aid et al., H1 collab., Nucl. Phys. **B480**, 3 (1996);
M. Arneodo et al., EMC collab., Phys. Lett. **B150**, 458 (1985);
M.R. Adams et al., E665 collab, Z. Phys. **C61**, 539 (1994).

[5] See, for example: D.H. Perkins, "Introduction to High Energy Physics", Addison-Wesley, Reading, 1982.

[6] A recent overview of the experimental status can be found for example in G. Mallot, proceedings of the "12th International Symposium on High Energy Spin Physics (SPIN '96)", 1996, Amsterdam, eds. C.W. de Jager et al., World Scientific (Singapore, 1997), p. 44.

[7] M. Gourdin, Nucl. Phys. **B38**, 418 (1972);
J. Ellis and R.L. Jaffe, Phys. Rev. **D9**, 1444 (1974); **D10**, 1669 (E) (1974).

[8] M. Burkardt and R.L. Jaffe, Phys. Rev. Lett. **70**, 2537 (1993).

[9] R.L. Jaffe and X. Ji, Phys. Rev. Lett. **71**, 2547 (1993);
X. Ji, Phys. Rev. **D49**, 114 (1994);
W. Lu, X. Li, and H. Hu, Phys. Rev. **D53**, 131 (1996).

[10] D. Buskulic et al., ALEPH collab., Phys. Lett. **B374**, 319 (1996); paper submitted to the "XVIII International Symposium on Lepton Photon Interactions", 1997, Hamburg, Germany, paper no. **LP279**.

[11] DELPHI collab., DELPHI 95-86 PHYS 521 (paper submitted to the EPS-HEP 95 conference, Brussels, 1995).

[12] K. Ackerstaff et al., OPAL collab., CERN-PPE/97-104, `hep-ex/9708027`.

[13] G.R. Court, HERMES collab., private communication.

[14] G. Baum et al., COMPASS collab., CERN/SPSLC 96-14.

[15] Among other conceivable upgrades, such an option is currently under discussion, see, for example: proceedings of the 1995/96 workshop on "Future Physics at HERA", Hamburg, Germany, eds. G. Ingelman, A. De Roeck, and R. Klanner.

[16] I. Bigi, Nuovo Cim. **41A**, 43 (1977); ibid. 581;
G. Gustafson and J. Häkkinen, Phys. Lett. **B303**, 350 (1993);
M. Nzar and P. Hoodbhoy, Phys. Rev. **D51**, 32 (1995).

[17] A. Bravar, A. Kotzinian, and D. von Harrach, `hep-ph/9701384`.

[18] R.L. Jaffe, Phys. Rev. **D54**, 6581 (1996).

[19] M. Stratmann and W. Vogelsang, Nucl. Phys. **B496**, 41 (1997).

[20] G. Altarelli, R.K. Ellis, G. Martinelli, and S.Y. Pi, Nucl. Phys. **B160**, 301 (1979);
P. Nason and B. Webber, Nucl. Phys. **B421**, 473 (1994); **B480**, 755 (E) (1996).

[21] W. Furmanski and R. Petronzio, Z. Phys. **C11**, 293 (1982).

[22] G. Curci, W. Furmanski, and R. Petronzio, Nucl. Phys. **B175**, 27 (1980);
W. Furmanski and R. Petronzio, Phys. Lett. **97B**, 437 (1980);

L. Beaulieu, E.G. Floratos, and C. Kounnas, Nucl. Phys. **B166**, 321 (1980);
P.J. Rijken and W.L. van Neerven, Nucl. Phys. **B487**, 233 (1997);
J. Binnewies, B.A. Kniehl, and G. Kramer, `hep-ph/9702408`.

[23] M. Glück, E. Reya, and A. Vogt, Phys. Rev. **D48**, 116 (1993); **D51**, 1427 (E) (1995).

[24] R.K. Ellis, W.J. Stirling, and B.R. Webber, "QCD and Collider Physics", Cambridge University Press, 1996.

[25] M. Glück, E. Reya, and A. Vogt, Z. Phys. **C67**, 433 (1995).

[26] M. Glück, E. Reya, M. Stratmann, and W. Vogelsang, Phys. Rev. **D53**, 4775 (1996).

[27] K. Ackerstaff et al., OPAL collab., CERN-PPE/97-086, `hep-ex/9708020`.

[28] V. Ravindran, Nucl.Phys. **B490**, 272 (1997); Phys. Lett. **B398**, 169 (1997).

[29] L. Trentadue and G. Veneziano, Phys. Lett. **B323**, 201 (1993).

[30] D. Graudenz, Nucl. Phys. **B432**, 351 (1994).

[31] D. de Florian, C. García Canal, and R. Sassot, Nucl. Phys. **B470**, 195 (1996).

[32] D. de Florian and R. Sassot, Nucl. Phys. **B488**, 367 (1997).

[33] For a study on polarized Λ production in the target fragmentation region of DIS see:
J. Ellis, D. Kharzeev, and A. Kotzinian, Z. Phys. **C69**, 467 (1996).

[34] M. Stratmann, Ph.D. Thesis, Univ. Dortmund report DO-TH 96/24 (unpublished).

[35] R.D. Ball, A. Deshpande, S. Forte, V.W. Hughes, J. Lichtenstadt, and G. Ridolfi, proceedings of the 1995/96 workshop on "Future Physics at HERA", Hamburg, Germany, eds. G. Ingelman, A. De Roeck, and R. Klanner, p. 777.

[36] A. De Roeck, private communication.

[37] K. Ackerstaff et al., HERMES collab., Phys. Lett. **B404**, 383 (1997).

[38] W. Lu and B.-Q. Ma, Phys. Lett. **B357**, 419 (1995);
W. Lu, Phys. Lett. **B373**, 223 (1996).

[39] G. 't Hooft and M. Veltman, Nucl. Phys. **B44**, 189 (1972);
P. Breitenlohner and D. Maison, Comm. Math. Phys. **52**, 11 (1977).

[40] W. Vogelsang, Phys. Rev. **D54**, 2023 (1996); Nucl. Phys. **B475**, 47 (1996).

[41] R.K. Ellis, M.A. Furman, H.E. Haber, and I. Hinchliffe, Nucl. Phys. **B173**, 397 (1980).

Figure Captions

Fig. 1 Comparison of our LO and NLO results for $(1/\sigma_{tot})d\sigma/dx_E$ according to Eq. (5) with all available data on unpolarized Λ production in e^+e^- annihilation [2, 3]. Note that only data points with $x_E \geq 0.1$ have been included in our fit (see text).

Fig. 2 z-dependence of our LO and NLO fragmentation functions as specified in Eq. (23) and Table 1 at $Q^2 = 100$ and $Q^2 = 10^4$ GeV^2.

Fig. 3 Q^2-dependence of our LO and NLO q and g fragmentation functions at fixed $z = 0.05, 0.1, 0.5$.

Fig. 4 Comparison of LEP data [10-12] and our LO and NLO results for the asymmetry A^Λ in (26), using the three different scenarios as described in the text.

Fig. 5 LO and NLO partonic fragmentation asymmetries $A_f \equiv \Delta D_f^\Lambda / D_f^\Lambda$ for $f = s$, $u = d$, and g at $Q^2 = 10\,\mathrm{GeV}^2$. In the LO plot we also show (dot-dashed lines) the effect of assuming a maximally polarized gluon distribution at the initial scale for scenario 1. The NLO results in this case are very similar to the LO ones and are therefore not shown.

Fig. 6 a) Compilation of the original SIDIS data [4] in terms of x_F. b) Comparison of our LO predictions with the data converted to the variable z (see text).

Fig. 7 LO and NLO predictions for the SIDIS asymmetry for unpolarized protons and polarized Λ's and leptons (see text) for our three distinct scenarios of polarized fragmentation functions. In a) we also show the expected statistical errors for such

a measurement at HERA, assuming a luminosity of $500\,\mathrm{pb}^{-1}$, a beam polarization of 70%, and a Λ detection efficiency of 0.1. In b) we include the expectation for scenario 1 with a maximal gluon polarization at the initial scale.

Fig. 8 The same as in Fig. 7, but now for HERMES kinematics.

Fig. 9 LO and NLO predictions for the SIDIS asymmetry for polarized protons but unpolarized leptons for two different sets of polarized parton distributions taken from [26]. Also shown are the expected statistical errors for such a measurement at HERA, calculated for the parameters already used for Fig. 7.

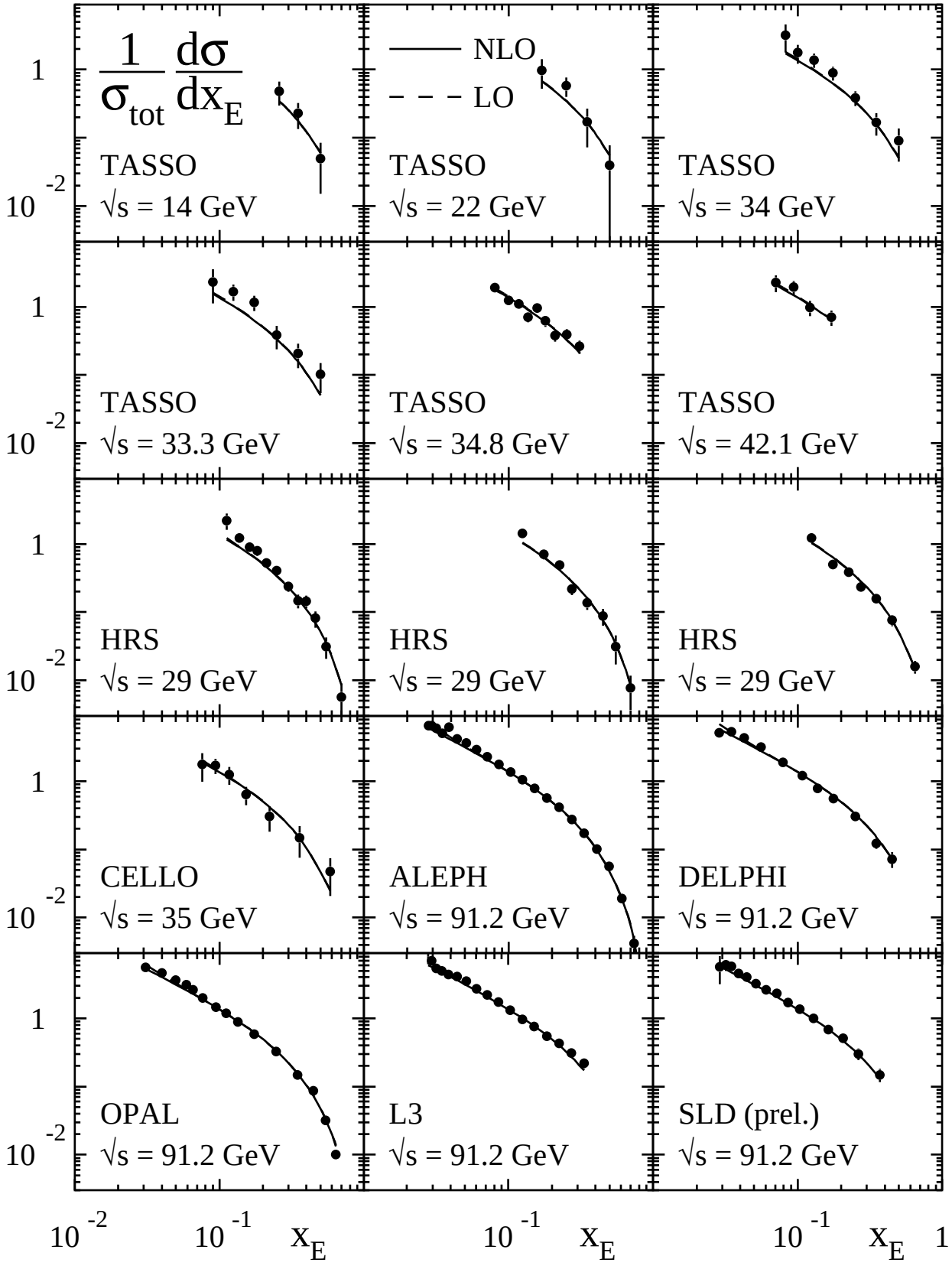
1/σ_tot dσ/dx_E
NLO
LO
TASSO
√s = 14 GeV
TASSO
√s = 22 GeV
TASSO
√s = 34 GeV
TASSO
√s = 33.3 GeV
TASSO
√s = 34.8 GeV
TASSO
√s = 42.1 GeV
HRS
√s = 29 GeV
HRS
√s = 29 GeV
HRS
√s = 29 GeV
CELLO
√s = 35 GeV
ALEPH
√s = 91.2 GeV
DELPHI
√s = 91.2 GeV
OPAL
√s = 91.2 GeV
L3
√s = 91.2 GeV
SLD (prel.)
√s = 91.2 GeV
1
10^-2
10^-1
1
x_E

Fig. 1

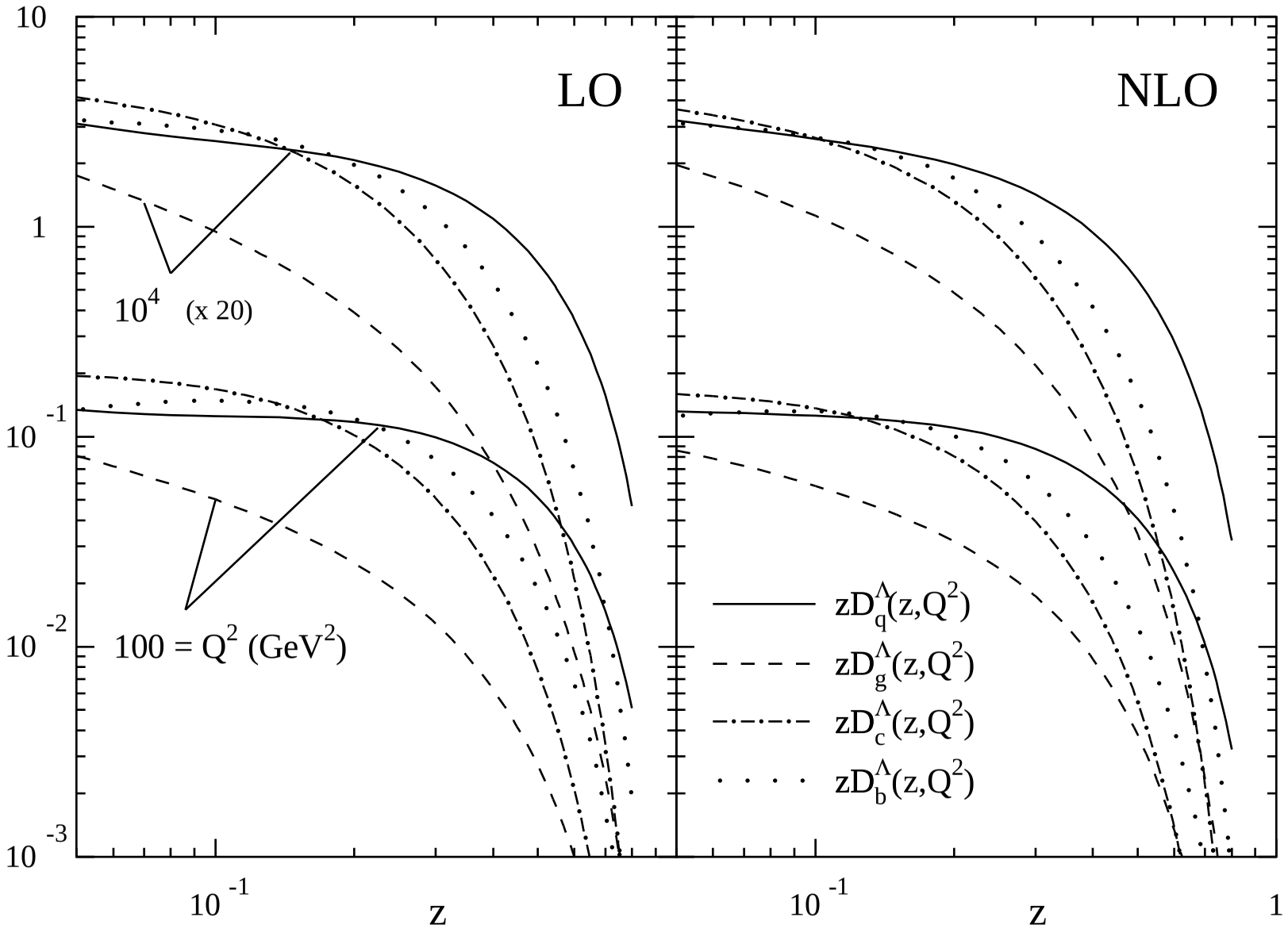
LO
NLO
10
1
10^-1
10^-2
10^-3
10^4 (x 20)
100 = Q^2 (GeV^2)
zD_q^Λ(z,Q^2)
zD_g^Λ(z,Q^2)
zD_c^Λ(z,Q^2)
zD_b^Λ(z,Q^2)
10^-1
z
10^-1
z
1

Fig. 2

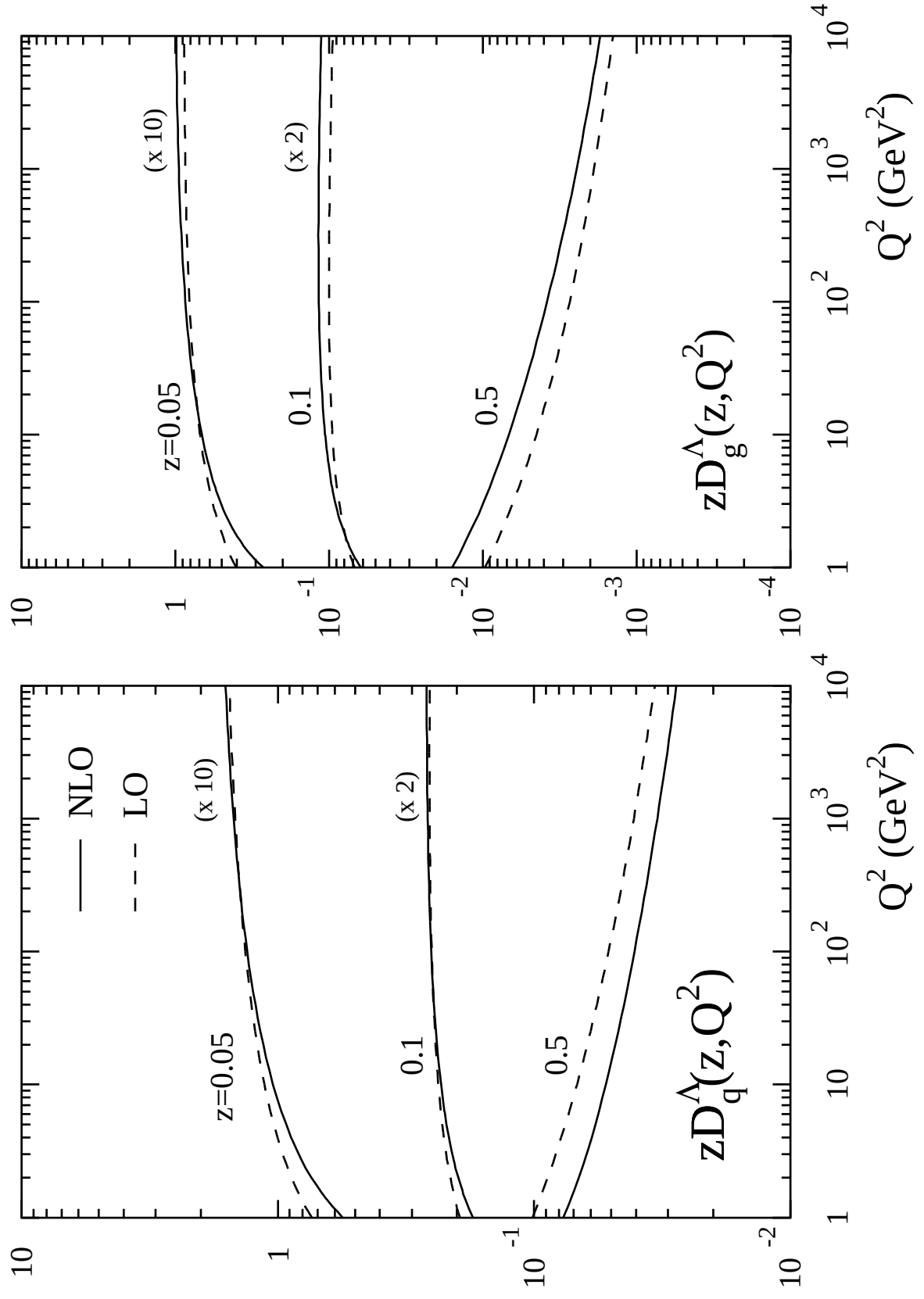

Fig. 3

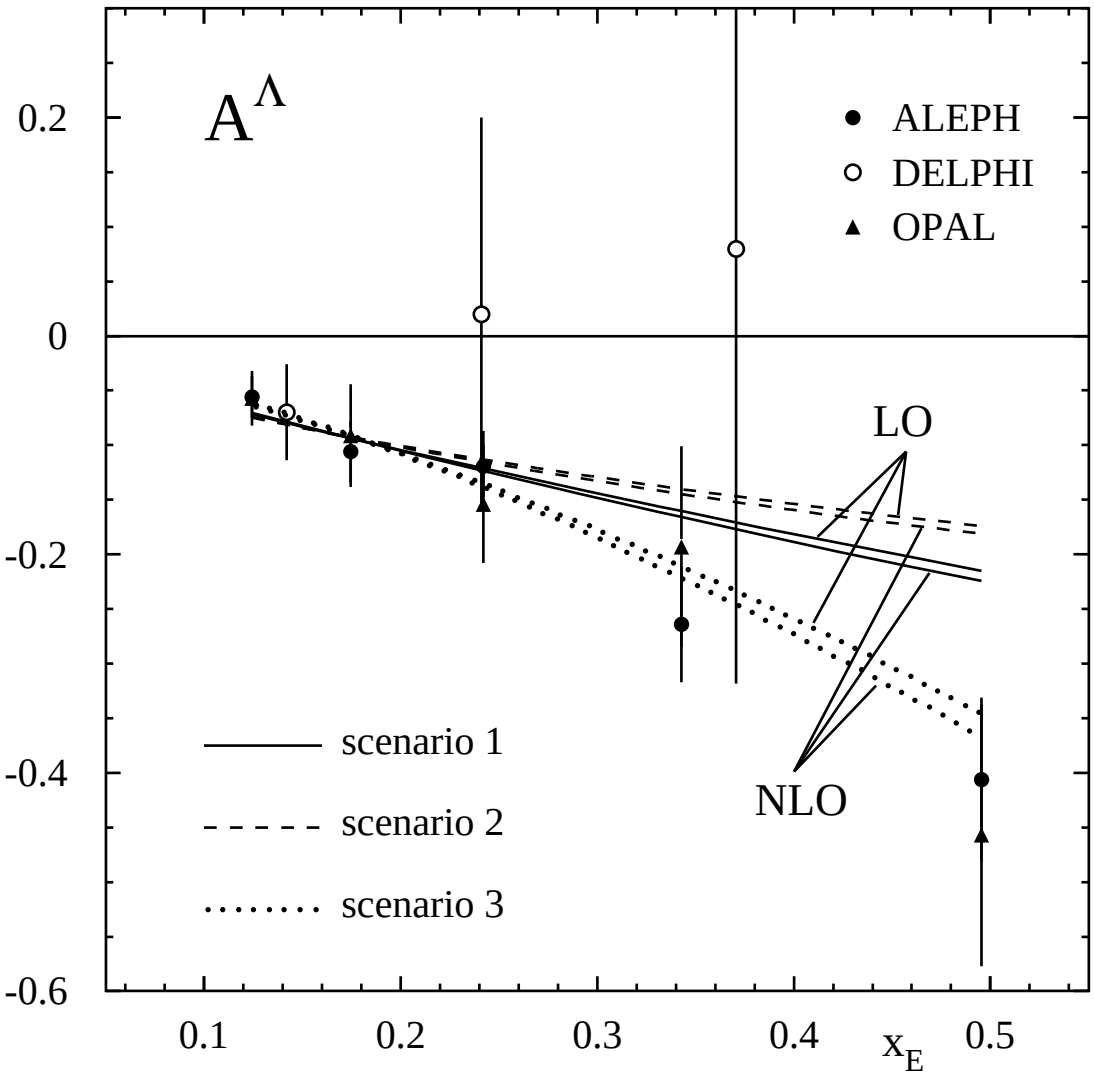
A^{Λ}
ALEPH
DELPHI
OPAL
LO
NLO
scenario 1
scenario 2
scenario 3
0.2
0
-0.2
-0.4
-0.6
0.1
0.2
0.3
0.4
0.5
x_E

Fig. 4

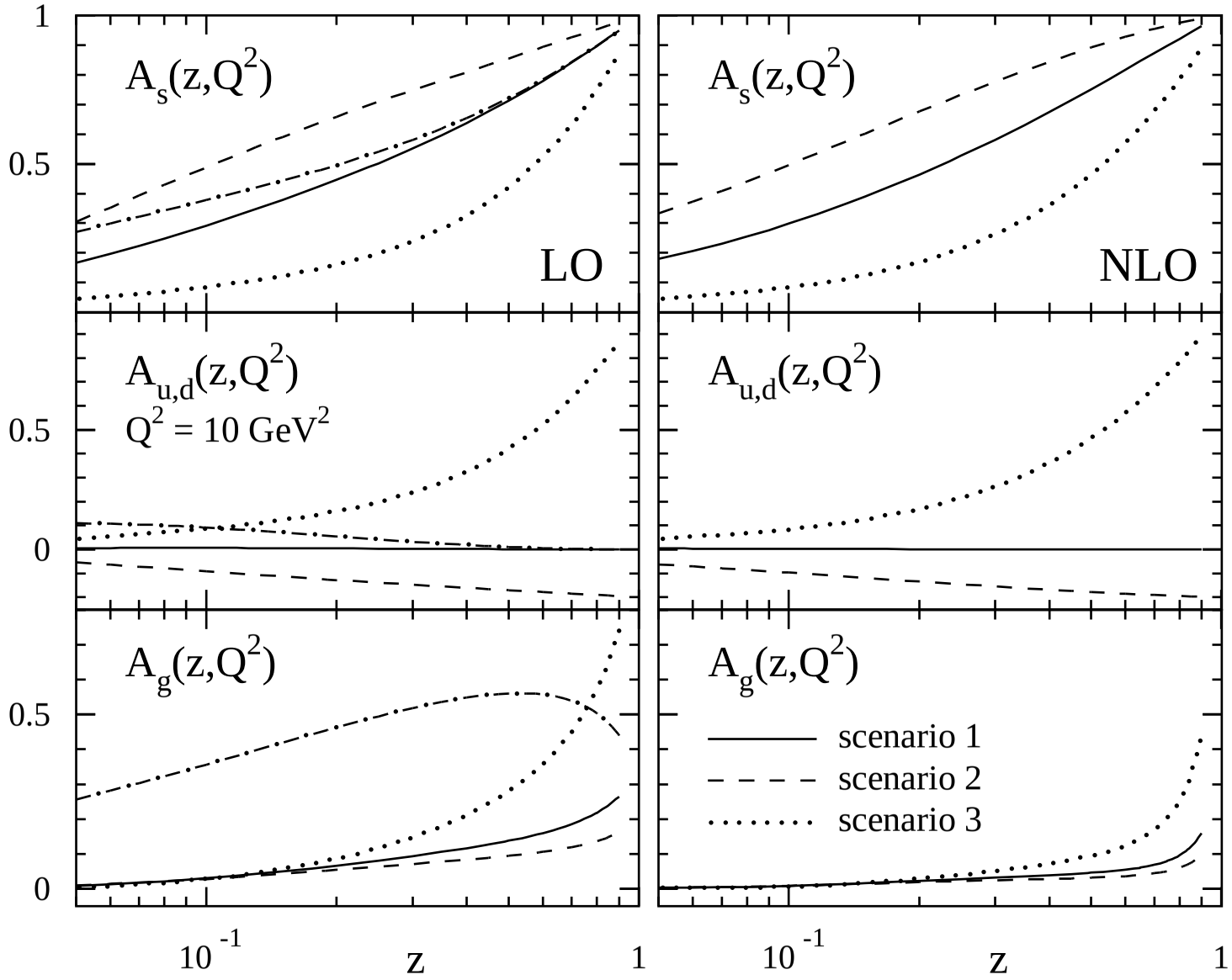
1
0.5
$A_s(z,Q^2)$
LO
$A_s(z,Q^2)$
NLO
$A_{u,d}(z,Q^2)$
$Q^2 = 10\ GeV^2$
0.5
0
$A_{u,d}(z,Q^2)$
$A_g(z,Q^2)$
0.5
0
$A_g(z,Q^2)$
scenario 1
scenario 2
scenario 3
10^{-1}
z
1
10^{-1}
z
1

Fig. 5

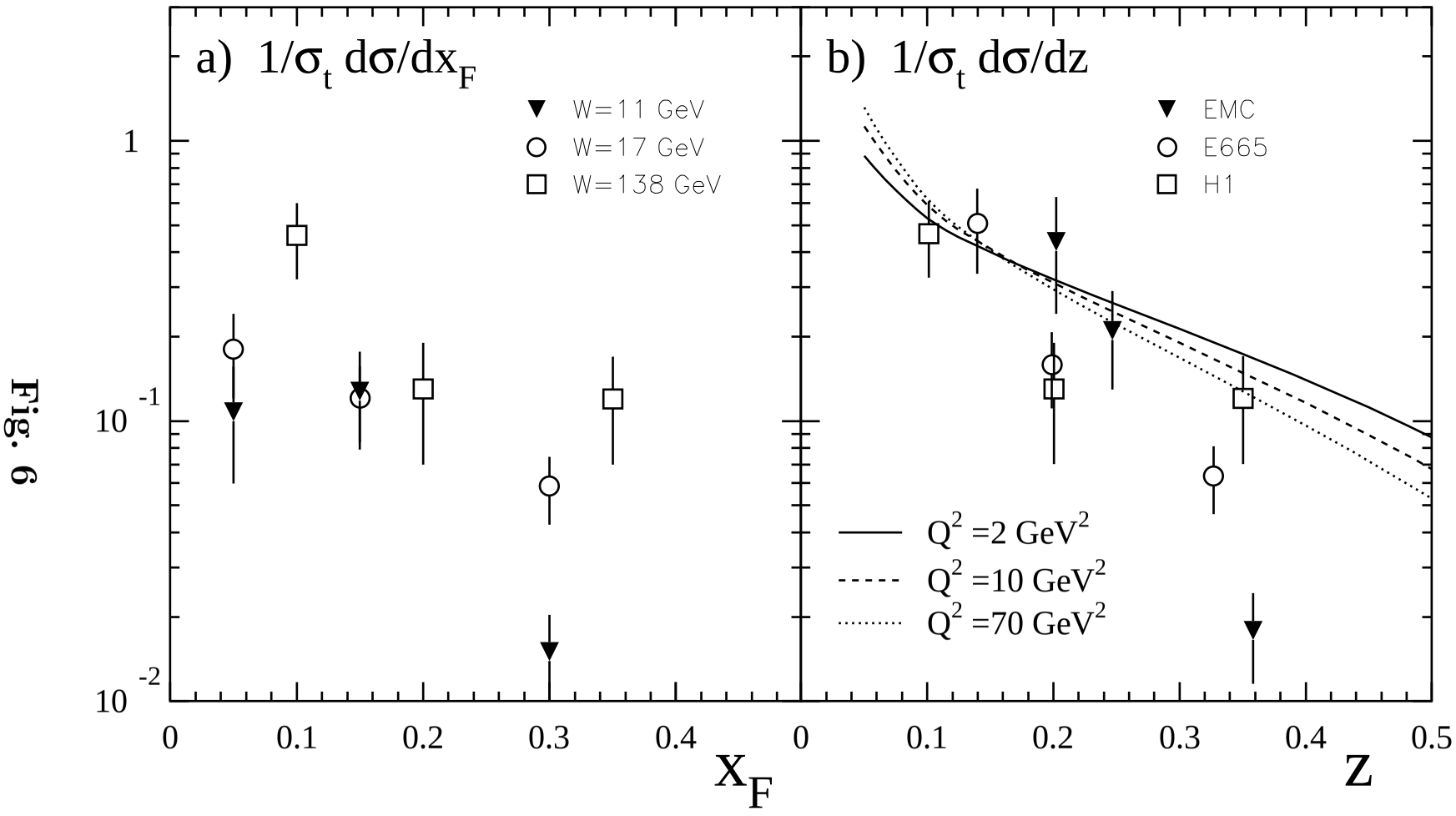
a) 1/σ_t dσ/dx_F
W=11 GeV
W=17 GeV
W=138 GeV
1
10^-1
10^-2
0
0.1
0.2
0.3
0.4
x_F
b) 1/σ_t dσ/dz
EMC
E665
H1
Q^2 =2 GeV^2
Q^2 =10 GeV^2
Q^2 =70 GeV^2
0
0.1
0.2
0.3
0.4
0.5
z

Fig. 6

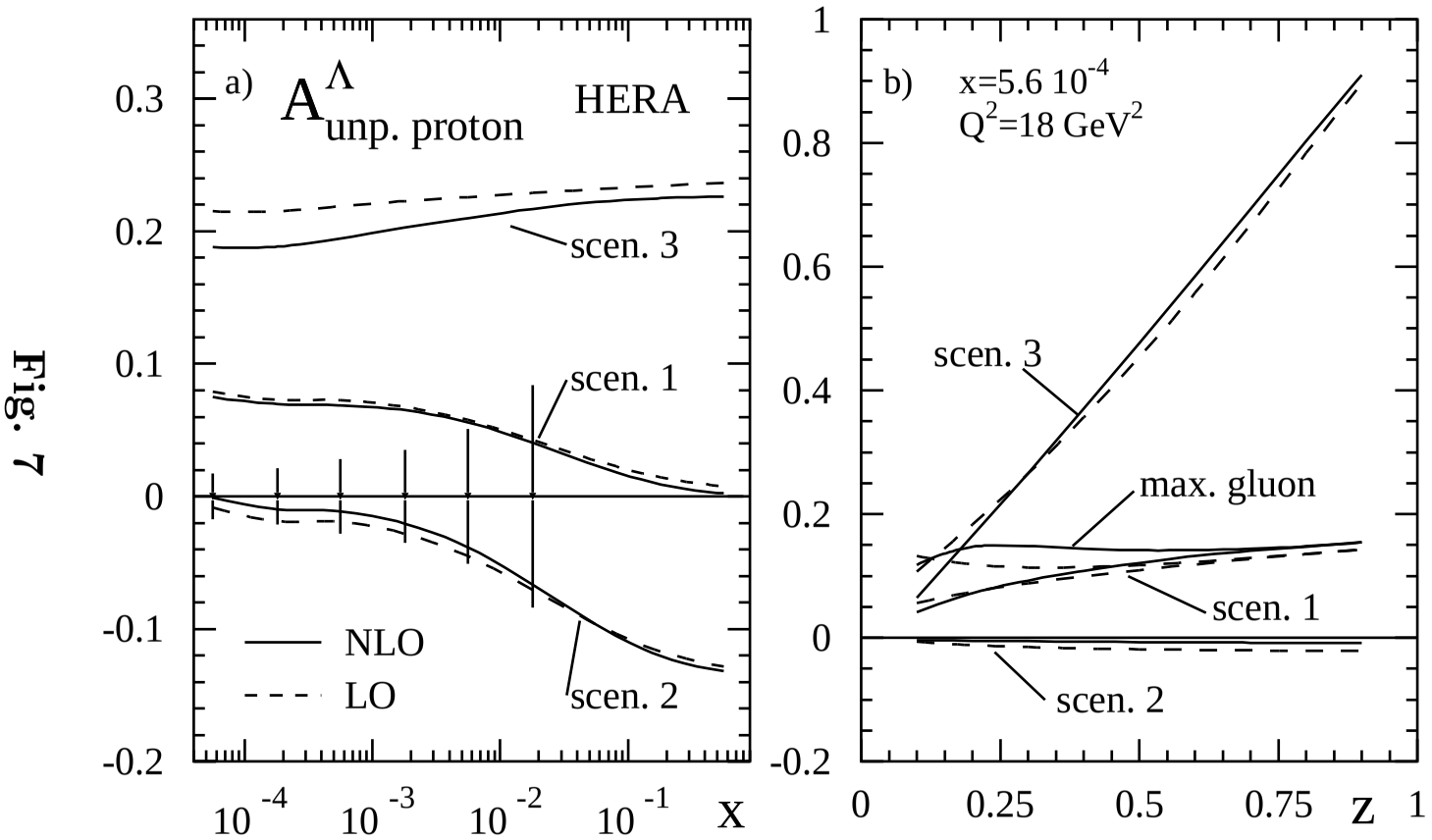
a)
$A^{\Lambda}_{unp.\ proton}$
HERA
scen. 3
scen. 1
scen. 2
NLO
LO
0.3
0.2
0.1
0
-0.1
-0.2
10^{-4}
10^{-3}
10^{-2}
10^{-1}
x
b)
$x=5.6\ 10^{-4}$
$Q^2=18\ GeV^2$
scen. 3
max. gluon
scen. 1
scen. 2
1
0.8
0.6
0.4
0.2
0
-0.2
0
0.25
0.5
0.75
z
1

Fig. 7

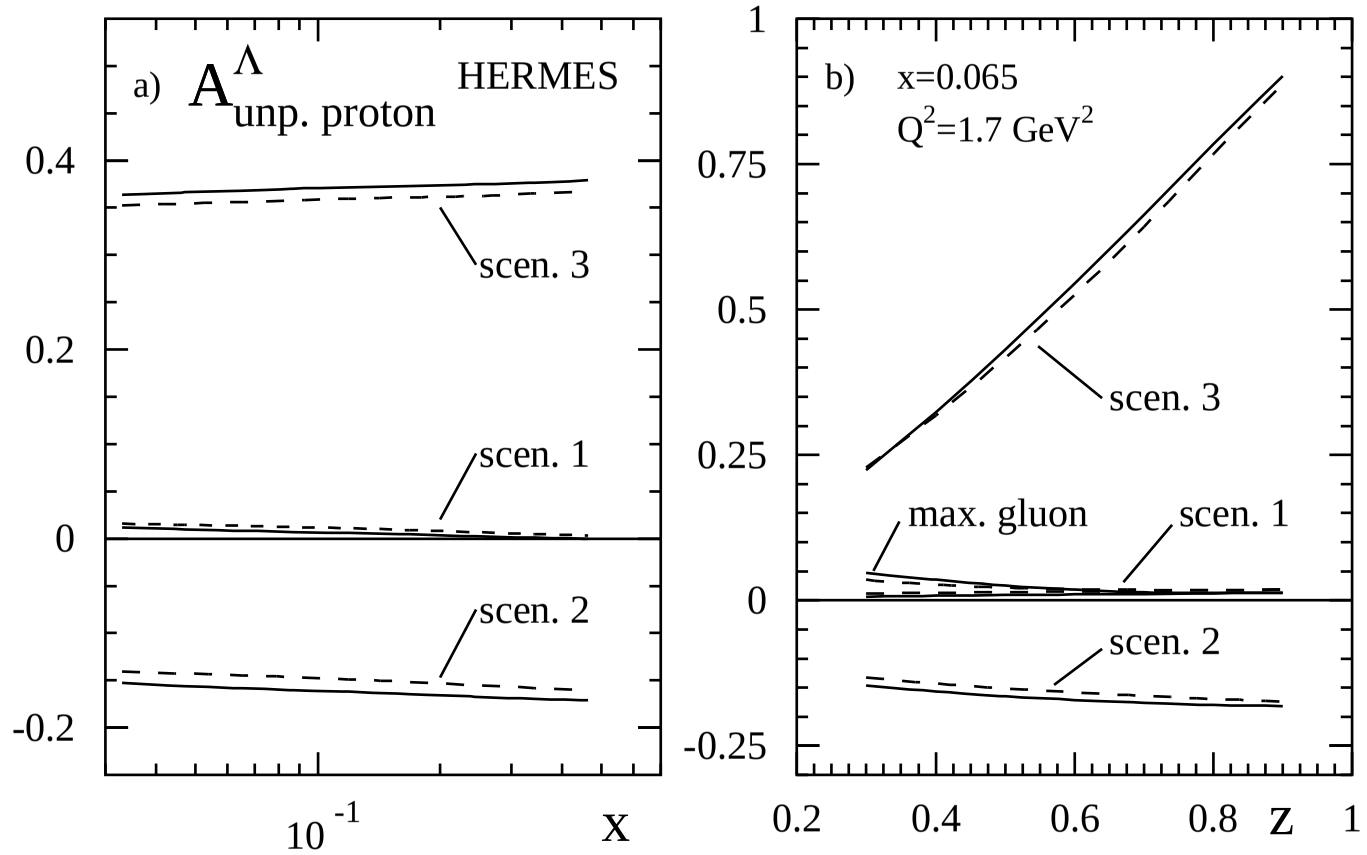
a)
$A^{\Lambda}_{unp.\ proton}$
HERMES
0.4
0.2
0
-0.2
scen. 3
scen. 1
scen. 2
10^{-1}
x
b)
x=0.065
Q^2=1.7 GeV^2
1
0.75
0.5
0.25
0
-0.25
scen. 3
max. gluon
scen. 1
scen. 2
0.2
0.4
0.6
0.8
z
1

Fig. 8

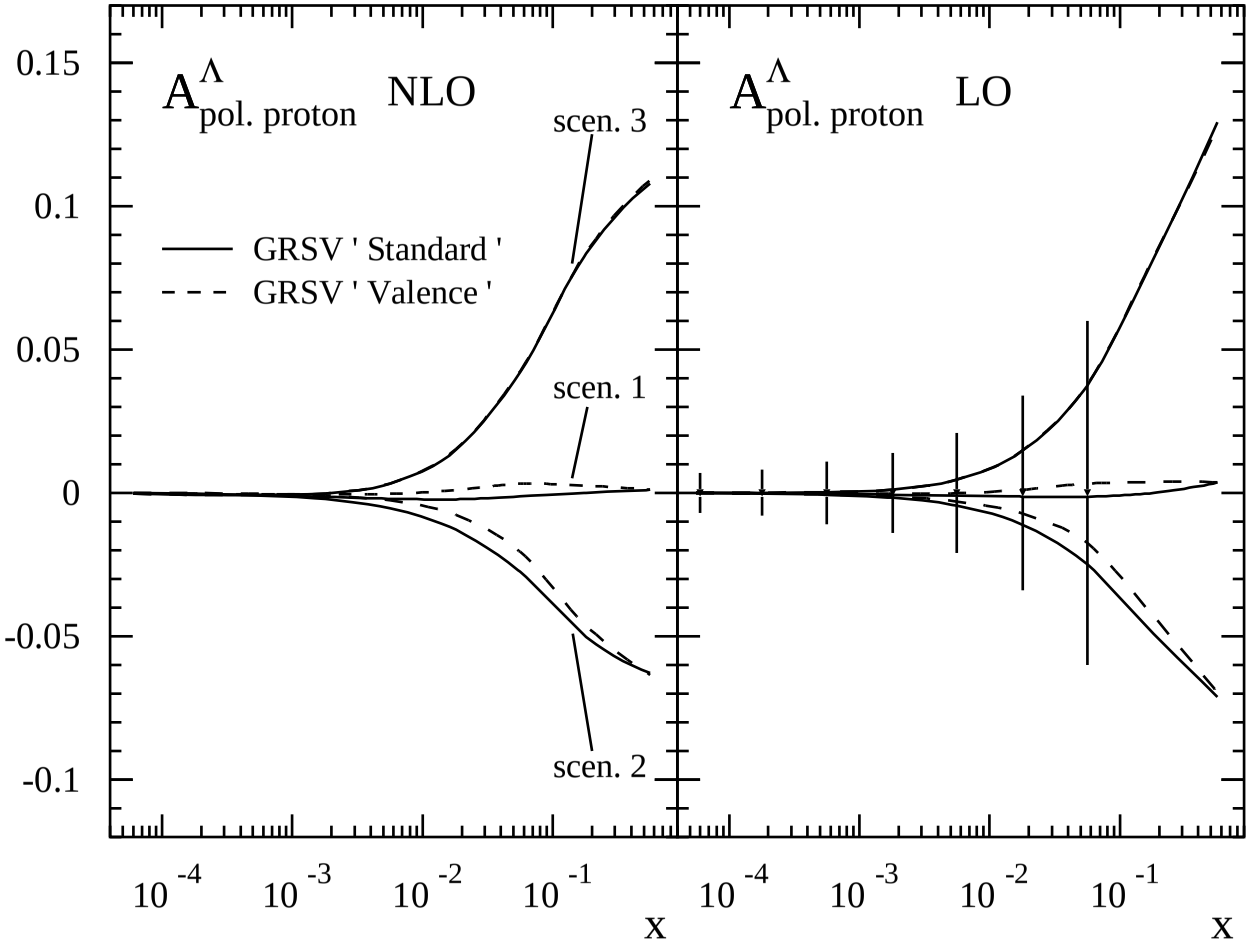
$A^{\Lambda}_{\text{pol. proton}}$ NLO
$A^{\Lambda}_{\text{pol. proton}}$ LO
GRSV ' Standard '
GRSV ' Valence '
scen. 3
scen. 1
scen. 2
0.15
0.1
0.05
0
-0.05
-0.1
10^{-4}
10^{-3}
10^{-2}
10^{-1}
x

Fig. 9